Transient Plume Impingement Analysis For Formation Flying Spacecraft

Michael Woronowicz

Swales Aerospace, 5050 Powder Mill Road, Beltsville, Maryland 20705, USA

Abstract. A study was performed to determine the impact of monopropellant hydrazine attitude control thruster operations as plume impingement fluxes between individual scientific spacecraft orbiting in formation as the proposed NASA/ESA "A-Train." Due to a combination of brief firing periods, large mean free path lengths, and large separation distances between spacecraft, a set of analytic point source transient free molecule equations was used to estimate interaction effects. Interesting observations include radial and angular variations on the approach to steady conditions with relative location, and the impact of species separation effect on transient impingement, including a surprisingly long-term persistence for lightweight species.

INTRODUCTION

There is a growing trend for space agencies to create programs featuring multiple scientific satellites operating in closely coordinated orbits. Such groups may orbit over the same ground track from Low Earth Orbit (LEO) in order to combine observations involving identical locations over a short period of time[1], to control individual satellite positions for making simultaneous measurements at different locations[2,3], or to measure fluctuations in the ambient environment experienced by individual spacecraft at different intervals of time and location[4]. Often, in "formation flying" mode, the relative positions of these spacecraft are precisely controlled using brief operations of chemical reaction control thrusters.

Another scenario occurs when spacecraft separate from their upper stages in orbit and the latter system is maneuvered away from the payloads for safety's sake, as in the Breeze-KM upper stage deorbit maneuver after jettisoning the GRACE spacecraft pair[5], or for Space Shuttle maneuvering after payload release or upon leaving a space station.

In these arrangements, program managers are concerned that thruster operations from one spacecraft may create non-negligible impingement effects on others. Furthermore, the combination of thruster pulse durations and distances between satellites may mean the impingement effects from these plumes should be modeled as transient events rather than in a steady-state fashion.

Due to the high level of rarefaction outside of the lowest reaches of LEO, mean free path lengths between the ambient atmosphere and thruster gases may be large enough to consider modeling the transient plume expansion using free molecule concepts as a first approximation.

This paper describes analyses performed using such a technique[6] for studying interactions within the "A-Train"[1], an international formation of as many as seven earth observation satellites orbiting at 705 km altitude in a sun-synchronous orbit, taking 30 min to pass over a given position. The model uses solutions of the collisionless Boltzmann equation due to point source expansions having a single velocity constraint for Delta function pulses and Heaviside step functions in mass flow rate[6].

BACKGROUND

Satellite Parameters

A NASA/ESA effort to operate a heterogeneous group of scientific satellites in a coordinated effort to make near-simultaneous atmospheric measurements over an identical ground track has been dubbed the "Afternoon Constellation," or "A-Train," after the lead spacecraft's 1:15 PM equator crossing time. This enhanced formation flying concept is currently planned to consist of six satellites, including OCO, Aqua (lagging by 15 min.), CloudSat (16 min.), CALIPSO (16.25 min.), PARASOL (17.25 min.), and Aura (30 min.)[1]. In addition, the Glory satellite is being considered for incorporation into the A-Train in 2008, lagging OCO by 20 min.

Relative distances between spacecraft may be determined from lag times, since at 705 km, orbital velocity V_∞ = 7.5 km/s, which corresponds to about 450 km per minute. Because the satellites follow the same ground track, and Earth rotates about 0.25 °/min., they do not lie precisely behind one another. Aura would lie about 7.5° off the aft normal from OCO.

Thruster Parameters

The satellites' Attitude Control Systems (ACS) are comprised of sets of aft-facing monopropellant thrusters, ranging from 1 N to 1 lb_f in thrust, and with maximum firing durations lasting from about 7 – 100 s, depending on the spacecraft. Plume species were based on 100 percent decomposition of high-purity grade monopropellant hydrazine with 65 percent ammonia decomposition[7], adding 0.5 percent mass fraction of water vapor as a system impurity. A nozzle exit velocity V_e = 2.2 km/s was used, with a mass flow rate $\dot{m}$ of 2.0 g/s per lb_f thrust. Exit profiles provided had been determined analytically, using an approach developed by Bartz[8]. These were expanded to produce conditions on a stubby, cylindrical starting surface meant to include expansion around the nozzle lip into the backflow regime, capped by a disk dominated by the bulk, core conditions aligned with the plume axis.

Flow Regime Determination

In order to determine the degree of rarefaction associated with this system, it is instructive to compute the average distance plume molecules travel between collisions with the ambient atmosphere. Application of the MSISE-90 atmospheric model[9] generated estimates of atmospheric density for A-Train conditions of $n_\infty \approx 2.1\times10^{11}$ molecules/m^3 (±5×), made up of over 99 percent atomic oxygen. Using the definition of mean free path length λ as the ratio of average molecular velocity divided by the relevant collision frequency[10]:

$$\lambda_{p-\infty,\,\lim} = \frac{V_e}{n_\infty \left| V_e \pm V_\infty \right| \sigma} . \tag{1}$$

For an average molecular diameter of about 0.3 nm, collision cross section $\sigma \approx 2.9\times10^{-19}$ m^2, and $\lambda_{p-\infty}$ = 3760 km in the ram direction and 6950 km in the wake. Since the A-Train operates at 705 km, clearly there will be an overwhelming level of interaction in the lower reaches of the atmosphere, and the plume will not develop symmetrically with altitude.

At 705 km altitude conditions, plume-ambient scattering occurs so infrequently relative to the time of flight between closest A-Train spacecraft, the ambient atmosphere arguably does not disturb the developing plume greatly, particularly for plume impingement on trailing satellites, and one may consider using molecular flow modeling to study these effects. Of course the effect of these collisions, particularly in the ram direction and for the most distant separations, is to scatter the plume molecules from their line-of-sight trajectories, causing the plume to diffuse. Therefore one should consider a molecular flow model to provide a degree of conservatism relative to the actual transport process.

In addition, due to the short ACS firing intervals relative to the distances separating A-Train spacecraft, it might not be adequate to assume steady conditions for determining surface flux couplings. In the most extreme case, the peak of fluxes from a 100 s plume generated in the wake of OCO would take one hour, 43 minutes to reach Aura! Therefore a transient molecular flow model has been employed to predict this behavior.

In addition to neglecting scattering occurring via ambient conditions at 705 km altitude, the effects of stratification of atmospheric density with altitude and solar ionization have been neglected, making this study a first approximation to actual impingement behavior. The analysis ignored the actual presence of the spacecraft, which would have provided considerable shielding for upwind satellites. This simplification adds another degree of conservatism to the analysis.

MODEL FORMULATION

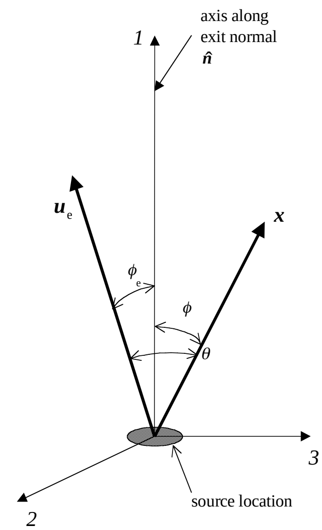

FIGURE 1. Schematic representation of various quantities and angles used in analytic model.

A transient solution of the collisionless Boltzmann equation was developed[6,11-13] to describe the molecular distribution $f(x,t)$ for flow from a point source step function Q_1 having a single velocity constraint, where

$$\frac{\partial f}{\partial t}+\boldsymbol{v}\cdot\frac{\partial f}{\partial \boldsymbol{x}}=Q_1; \qquad Q_1=\frac{2\beta^4}{A_1\pi}\delta(\boldsymbol{x})\dot{m}(t)\left|\boldsymbol{v}\cdot\hat{\boldsymbol{n}}\right|\exp\left(-\beta^2(\boldsymbol{v}-\boldsymbol{u}_\mathrm{e})^2\right)$$
$$A_1\equiv e^{-s^2\cos^2\phi_\mathrm{e}}+\sqrt{\pi}\,s\cos\phi_\mathrm{e}\left(1+\mathrm{erf}\left(s\cos\phi_\mathrm{e}\right)\right) \tag{2}$$

Q_1 represents directed flow from a Lambertian, thermal velocity distribution superimposed on convective exit velocity $\boldsymbol{u}_\mathbf{e}$ for mass flow rate $\dot{m}$, $\beta\equiv 1/\sqrt{2RT}$, and speed ratio $s\equiv\beta u_\mathrm{e}$. Normal $\hat{\boldsymbol{n}}$ represents the orientation of a local starting surface element, and $\boldsymbol{v}\cdot\hat{\boldsymbol{n}}$ emphasizes the imposed directional constraint. Generally, $\boldsymbol{u}_\mathbf{e}$ is not aligned with $\hat{\boldsymbol{n}}$, with the angle between the two defined by ϕ_e. Local angle ϕ is measured between variable position $\boldsymbol{x}$ (distance r, experiencing local velocity $\boldsymbol{v}$) and $\hat{\boldsymbol{n}}$, and angle θ is measured between $\boldsymbol{u}_\mathbf{e}$ and $\boldsymbol{x}$.

The particular solution of Eq. (2) is found using approaches outlined by Bird[14] and Narasimha[15]. The density field generated for a step function in $\dot{m}$ is given by[13]

$$\rho(\boldsymbol{x},t)=\frac{\beta\,\dot{m}\cos\phi}{A_1\pi r^2}e^{w^2-s^2}\left\{(\alpha+w)e^{-z^2}+\left(\frac{1}{2}+w^2\right)\sqrt{\pi}\,\mathrm{erfc}\,z\right\}, \tag{3}$$

where $z\equiv\alpha-w$, $\alpha\equiv\beta r/t$, and $w\equiv s\cos\theta$. Solving for successive velocity moments, one finds mass flux $\dot{\Phi}$, incident normal momentum flux $p_\perp$, and incident translational energy flux $\dot{q}_\mathrm{TR}$:

$$\dot{\Phi}(\boldsymbol{x},t)=\frac{\dot{m}\cos\phi}{A_1\pi r^2}\frac{\boldsymbol{x}}{r}e^{w^2-s^2}\left\{\left(\alpha^2+\alpha w+w^2+1\right)e^{-z^2}+\left(\frac{3}{2}+w^2\right)\sqrt{\pi}\,w\,\mathrm{erfc}\,z\right\}, \tag{4}$$

$$\tilde{p}_\perp(\boldsymbol{x},t)=\frac{\dot{m}\cos\phi}{\beta A_1\pi r^2}e^{w^2-s^2}\left\{\left(\alpha^3+\alpha^2 w+\alpha w^2+w^3+\frac{5}{2}w+\frac{3}{2}\alpha\right)e^{-z^2}+\left(\frac{3}{4}+3w^2+w^4\right)\sqrt{\pi}\,\mathrm{erfc}\,z\right\}, \tag{5}$$

$$\begin{aligned}\dot{q}_{\mathrm{TR}}(\boldsymbol{x},t)=&\frac{\dot{m}\cos\phi}{2\beta^2 A_1\pi r^2}\frac{\boldsymbol{x}}{r}e^{w^2-s^2}\\&\times\left\{\left(\alpha^4+\alpha^3 w+\alpha^2 w^2+\alpha w^3+w^4+2\alpha^2+\frac{7}{2}\alpha w+\frac{9}{2}w^2+2\right)e^{-z^2}\right.\\&\left.+\left(\frac{15}{4}+5w^2+w^4\right)\sqrt{\pi}\,w\,\mathrm{erfc}\,z\right\}.\end{aligned} \tag{6}$$

Eq. (5) becomes normal momentum flux $p_\perp$ when multiplied by the dot product $\boldsymbol{x}$ makes with the local normal of the impinged surface. Eqns. (3)-(5) may be combined to obtain expressions for velocity $\boldsymbol{v}$, translational temperature T_{TR}, and internal energy flux $\dot{q}_{\mathrm{INT}}$ for polyatomic molecules having specific heat ratio γ:

$$\boldsymbol{v}(\boldsymbol{x})=\frac{\dot{\Phi}(\boldsymbol{x})}{\rho(\boldsymbol{x})};\qquad T_{\mathrm{TR}}(\boldsymbol{x})=\frac{1}{3R}\left\{\frac{\tilde{p}_\perp(\boldsymbol{x})}{\rho(\boldsymbol{x})}-\left(\boldsymbol{v}(\boldsymbol{x})\right)^2\right\};\qquad \dot{q}_{\mathrm{INT}}(\boldsymbol{x})=\left(\frac{5-3\gamma}{\gamma-1}\right)\frac{\dot{\Phi}(\boldsymbol{x})}{4\beta^2}. \tag{7}$$

Reflected quantities such as normal momentum flux and energy are found by setting s = 0, letting $\hat{\boldsymbol{n}}$ represent the local surface element, and assuming the mass flux to a surface element is conserved[14]. The expansion around the nozzle lip into the backflow region may be portrayed by using the near field solution of a continuum code to create a starting surface for a network of FM point sources having locally varying conditions.

When the constant mass rate $\dot{m}$ in Eq. (2) is replaced by a Dirac Delta function $\Delta m\,\delta(t)$, a simpler set of velocity moments is produced to describe pulse flowfields.

$$\rho(\boldsymbol{x},t)=\frac{2\,\Delta m\beta^4}{A_1\pi}\frac{r\cos\phi}{t^4}e^{w^2-s^2}e^{-z^2};\ \ \dot{\Phi}(\boldsymbol{x},t)=\frac{\rho\,\boldsymbol{x}}{t};\ \ p_\perp(\boldsymbol{x},t)=\frac{\rho\,r^2}{t^2};\ \ \dot{q}_{\mathrm{TR}}(\boldsymbol{x},t)=\frac{\rho\,r^2\boldsymbol{x}}{2t^3}. \tag{8}$$

Convolution of these equations at constant strength reproduce the step function responses described by Eqns. (3)-(6).

In addition, one may create square wave responses by taking the difference of two step function sources of equal strength, where the second source has been shifted by ACS operational period. For much later time intervals, such solutions should evolve to complete agreement with their equivalent pulse source behavior.

RESULTS & DISCUSSION

A number of cases were studied in order to determine the impingement fluxes of a single ACS thruster firing on any A-Train spacecraft as it affected each of the others. Other cases were run in order to compare the transient development of pulse and brief square wave plume solutions to verify that they would merge to the same results at large time scales, and still other cases were run to observe how step function responses evolved into steady state solutions.

Regarding the approach to steady state, a time-lapsed succession of spatial contour maps were created for various plume quantities. Unsurprisingly, it was noticed that steady-state was approached more quickly for locations near the thruster than farther away. However, it was also clear that upstream locations continued to evolve after their downstream counterparts ceased such behavior. A review of the model and its implementation revealed why this was the case.

The $\boldsymbol{v} \cdot \hat{\boldsymbol{n}}$ velocity constraint in Eq. (2) forces the solution to be valid only over 2π steradians measured off the normal associated with each element of the starting surface. The parameter z tends to $-w = -s\cos\theta$, which becomes ever smaller as $\theta \to \pi/2$, compared to other spatial locations at the same radius, but more downstream. Upstream locations at very high angles off the surface normal and the local velocity vector are only influenced by the portion of the starting surface representing the boundary layer, and in this case the starting surface was a cylinder aligned with the nozzle axis. These details combine to produce longer-term transients upstream than downstream. It would be interesting to verify whether such behavior has actually been observed in practice.

Returning to impinging fluxes due to satellite formation flying ACS thruster operations, attention will be focused on mass flux results from a 100 s, 1 lb_f, single-thruster operation from the Aqua spacecraft as experienced by other A-Train satellites (Fig. 2); the behavior of other fluxes is similar.

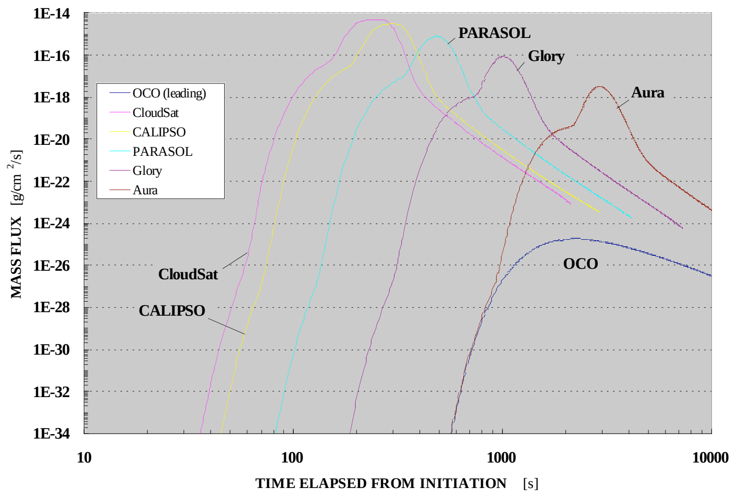

FIGURE 2. Transient mass flux profiles experienced by A-Train satellites due to Aqua thruster firing.

Aqua was selected as a source because it will lie at the center of the satellite formation, with OCO leading by 15 min. and Aura lagging by the same amount. The model impingement effect on these two spacecraft highlight the main differences between upstream and downstream behavior, respectively, which also can be dramatically observed in time-lapsed contour map movies of flux evolution in a plane containing the thruster axis.

For early times, fluxes experienced in either direction are similar, as wave-like term $\alpha \equiv \beta r/t$ dominates parameter z in Eqns. (3) – (6). However, upstream and downstream behavior diverge as time continues due to the bulk motion directed downstream, which is absent from the upstream ensemble.

Up to almost 2000 s after the Aqua thruster initiated firing, fluxes reaching OCO and Aura consisted entirely of molecular hydrogen. Subsequently a second phenomenon due to the species separation effect becomes apparent. At high degrees of rarefaction, lightweight species will tend to spread fairly diffusely while heavier species remain more tightly focused around the plume axis[16]. Due to the high upstream angle for gases reaching OCO from Aqua (176.25° off the Aqua thruster axis, 86.25° off the cylindrical portion of the source starting surface), the species separation effect ensures that fluxes reaching OCO are overwhelmingly due to H_2 at all times. For Aura however, NH_3, N_2, and impurity H_2O become increasingly present, and another, higher peak occurs, with a maximum value occurring very close to the time expected for a disturbance traveling at V_e to reach the spacecraft.

In Figure 2, transient fluxes from Aqua intercepted by the other lagging spacecraft reveal forms similar to Aura's. A plot for density indicates a maximum value of 2.3×10^{-20} g/cm^3 would be measured at CloudSat's position, which is roughly 0.3 percent of that for the ambient atmosphere.

The highest intercepted fluxes of any spacecraft thruster firings were obtained by CloudSat operations on CALIPSO, which nominally lags it by only 15 s (a distance of 112.5 km). With this model, a 19 s, 1-lb_f, single thruster operation would produce a maximum density level of 3.5×10^{-19} g/cm^3, or 4.5 percent of background levels.

CONCLUDING REMARKS

ACS thruster operations from each element of the NASA/ESA A-Train were modeled using a distributed point source, transient free molecule approach as a first approximation to determining impingement fluxes on each of the other members. For the planned combination of ACS operational periods and separation distances between successive spacecraft, the model showed that in no case would the use of steady conditions have been justified.

Results indicated for A-Train conditions that these interaction effects should be negligible, but with an increasing number of mission planners considering the formation flying concept, it should be expected that such scenarios will continue to be revisited.

ACKNOWLEDGEMENTS

The author gratefully acknowledges support from NASA Contract NAS5-01090 and Swales Aerospace.

REFERENCES

1. M. Taverna, *Aviation Week & Space Technology*, 14 June 2004, pp. 50-51.
2. M. Rhee *et al.*, "Highlights of Nanosatellite Propulsion Development Program at NASA-Goddard Space Flight Center," SSC-00-X-5, *Proceedings of the 14th AIAA/USU Conference on Small Satellites*, 2000.
3. A. Masson, "Five Years of Formation Flying with Cluster", <*http://sci.esa.int/science-e/www/object/index.cfm?fobjectid=37680*>, ESA, Noordwijk, 14 July 2005.
4. M. Walker, *Aerospace America*, December 2005, pp. 54-55.
5. *Eurockot User Guide*, Issue 4, Rev 0, Bremen, November 2004, pp. 2-6, 3-19, & 4-13.
6. M. Woronowicz, in *Proceedings of the 23rd Int.l Symposium on Rarefied Gas Dynamics*, American Institute of Physics, AIP Conf. Proceedings, **663**, Melville, NY, 588-95 (2003).
7. J. Genovese, "Rapid Estimation of Hydrazine Exhaust Plume Interaction," *AIAA Paper No. 78-1091*, presented at the AIAA/SAE 14th Joint Propulsion Conference, Las Vegas, NV 25-27 July 1978.
8. Bartz, D. R., "An Approximate Solution of Compressible Turbulent Boundary-Layer Development and Convective Heat Transfer in Convergent-Divergent Nozzles," *Transactions of the ASME*, November 1955, pp. 1235-1245.
9. A. Hedin, "Extension of the MSIS Thermospheric Model into the Middle and Lower Atmosphere," *J. Geophys. Res.*, **96**, 1159 (1991).
10. W. Vincenti, C. Kruger, *Introduction to Physical Gas Dynamics*, Robert E. Krieger Pub. Co., Malabar, FL, 1982, p. 13.
11. M. Woronowicz, D. Rault, "On Plume Flowfield Analysis and Simulation Techniques," *AIAA Paper No. 94-2048*, presented at the 6th AIAA/ASME Joint Thermophysics and Heat Transfer Conference, Colorado Springs, CO, 20-23 June 1994.
12. M. Woronowicz, in *Proceedings of the 22nd Intl. Symposium on Rarefied Gas Dynamics*, American Institute of Physics, AIP Conf. Proceedings **585**, Melville, NY, 798-805 (2001).
13. M. Woronowicz, in *Proceedings of the 24th Intl. Symposium on Rarefied Gas Dynamics*, American Institute of Physics, AIP Conf. Proceedings **762**, Melville, NY, 431-6 (2005).
14. G. A. Bird, *Molecular Gas Dynamics and the Direct Simulation of Gas Flows*, Clarendon Press, 1994, pp. 77-88.
15. R. Narasimha, "Collisionless expansion of gases into vacuum," *Journal of Fluid Mechanics*, **12**, 294-308 (1962).
16. G. Koppenwallner, "Species Separation in Rocket Exhaust Plumes and Analytic Plume Flow Models," invited paper, *Rarefied Gas Dynamics 22nd International Symposium*, Sydney, Australia, 9-14 July 2000, American Institute of Physics Conference Proceedings, **585**, Melville, NY, 797 (2001).